HyperCoal-derived porous carbons with alkaline hydroxides and carbonate activation for electric double-layer capacitors

Xiao-Yan Zhao [a], Shan-Shan Huang [a], Jing-Pei Cao [a,b,*], Xian-Yong Wei [a], Kazushi Magarisawa [b], Takayuki Takarada [b]

[a] Key Laboratory of Coal Processing and Efficient Utilization, Ministry of Education, China University of Mining & Technology, Xuzhou 221116, Jiangsu, China
[b] Division of Environmental Engineering, Gunma University, 1-5-1 Tenjin-cho, Kiryu 376-8515, Japan

ARTICLE INFO

ABSTRACT

Electrical double layer capacitors (EDLCs) with HyperCoal-derived activated carbons (ACs) as electrodes are reported in this work. The ACs were prepared by the carbonization of HyperCoal at 600 °C followed by the activation with KOH and NaOH for 2 h between 500 and 800 °C to achieve high total pore volume (TPV) and specific surface area (SSA). The porosity of the ACs was characterized with N_2 adsorption at 77 K. The results show that the ACs prepared with KOH and NaOH activations at 700 °C have a SSA of 2594 and 3010 $m^2\,g^{-1}$ and a TPV of 1.36 and 1.77 $cm^3\,g^{-1}$, respectively, leading to the highest specific capacitance of 43.1 and 43.9 $F\,g^{-1}$, respectively, in a two-electrode EDLC cell with 0.5 M tetraethylammonium tetrafluoroborate/propylene carbonate (TEABF$_4$/PC) electrolyte. Activations with $CaCO_3$ and KOH/$CaCO_3$ mixture were also investigated to understand the effect of $CaCO_3$ on the properties of the ACs. $CaCO_3$ significantly inhibited the porosity development during KOH activation and gave ACs with quite low SSA and specific capacitance. The results demonstrated that the alkaline hydroxide activation is an efficient approach to the preparation of ACs from HyperCoal with high-performance for EDLCs.

© 2014 Elsevier B.V. All rights reserved.

1. Introduction

Electric double-layer capacitor (EDLC) is an energy storage device that utilizes the electric double layer formed at the interface between the electrode and the electrolyte [1]. As an energy storage/conversion device, EDLC exhibits higher power density and longer cycling life than common batteries, and has much higher energy density compared with traditional dielectric capacitors [2,3]. At present, carbon materials, including activated carbons (ACs), carbon nanotubes, carbon nanofibers, and graphene sheets are widely used for EDLC electrode materials [3–6]. Especially, porous AC with a high specific surface area (SSA) has attracted significant interest due to their exceptional characteristics, such as moderate cost, good chemical stability, and high electrical conductivity.

The preparation conditions of the activation process can be changed largely, not only because there are many variables that affect the activation process, but also because of the variety of raw precursors and activating agents that can be used [7,8]. Chemical and physical activations are mostly used for AC preparation. Chemical activation is known as a single step method of preparation of AC in the presence of chemical agents. Among the chemical activation agents, KOH and NaOH are usually used because both the alkaline hydroxides can act as a dehydrating agent allowing more carbon to keep fixed for producing a well-developed porosity AC in high yield [9,10]. Alkaline hydroxide activation

can provide AC with a SSA higher than 2000 $m^2\,g^{-1}$ [2,11,12] and results in a quite high specific capacitance value when the AC was further used as EDLC electrode [13,14].

Generally, CO_2 and KOH activation can greatly promote the formation of micropores and small mesopores for providing high SSA of ACs [15]. It is well known that $CaCO_3$ can be decomposed to CO_2 at a high temperature [16]. Physical activation with CO_2 is a usual procedure for AC preparation [17]. Sato et al. [16] reported a simple fabrication route of ACs in high SSA from chicken droppings without any additional activation process and revealed that activation was achieved through the catalytic gasification with CO_2 evolved from decomposition of $CaCO_3$ in the droppings. However, the effect of $CaCO_3$ on the preparation of ACs is yet unclear at present. Furthermore, coal usually contains ash in carbonate form, such as $CaCO_3$, which should affect the performance of the obtained ACs simultaneously.

HyperCoal is an ashless coal obtained by a mild thermal extraction of coal (HyperCoal process), which eliminates the effects of ash and carbonates [18]. HyperCoal was reported to be an excellent and low-cost candidate for manufacturing ACs for high-performance electrodes of EDLC [19]. Nevertheless, it is yet necessary to optimize the preparation process, choosing the best activation agents and conditions to obtain the best capacitance performance. Some researchers [15] used KOH etching and CO_2 gasification to prepare porous ACs and found that the pore size distribution of the ACs was widened and the total pore volume (TPV) was increased, resulting in a high specific capacitance of 197 $F\,g^{-1}$ in 0.5 M H_2SO_4 aqueous electrolyte. $CaCO_3$ is desired to play a role in

physical activation when mixed with KOH. Addition of $CaCO_3$ during activation of HyperCoal is also important for understanding the effect of carbonates in coal on the performance of prepared ACs.

The aim of this work is to prepare high-performance ACs by two-step activation of HyperCoal in the presence of NaOH, KOH, $CaCO_3$, and KOH/$CaCO_3$ mixture for EDLC. The effects of activation temperature on the pore structure parameter and electrochemical performance of the resulting ACs for EDLC in 0.5 M tetraethylammonium tetrafluoroborate/propylene carbonate (TEABF$_4$/PC) electrolyte were addressed in detail.

2. Experimental

2.1. Material and reagents

The HyperCoal was provided by Kobe Steel, Ltd., in Japan. The production and main characteristics of the HyperCoal were described in detail previously [18,19]. The HyperCoal contains 0.03% of ash, 37.8% of volatile matter and 62.17% of fixed carbon (wt.%, dried basis). The elemental contents (wt.%, dried and ash-free basis) of C, H, N, S, and O are 83.5%, 5.4%, 2.2%, 0.6%, and 8.3%, respectively.

2.2. Preparation and characterization of ACs

Two-step activation was adopted for preparation of porous carbons. The HyperCoal was heated to 600 °C at 10 °C min^{-1} under Ar flow and carbonized at that temperature for 7 min. The carbonized residue was mixed with KOH, NaOH, $CaCO_3$, and KOH/$CaCO_3$ mixture at a certain weight ratio. The mixture was heated to a prescribed temperature between 500 and 800 °C and then held at that temperature for 2 h under Ar flow. After cooling down, the residue was washed with 2 M HCl and rinsed with distilled water until neutral and then dried in vacuum at 200 °C for 2 h. The preparation conditions and characterization of the resulting ACs are listed in Table 1. The ACs were designated as AX-Y, where A, Y, and X represent the activating agent, the activation temperature, and the mass ratio of activating agents/char, respectively.

The porous texture and the SSA of the ACs were characterized with nitrogen adsorption and desorption studies at 77 K in a BELSORP-max constant volume adsorption apparatus. A JEOL JEM-2010 transmission electron microscope (TEM) was employed for AC characterization.

2.3. Determination of specific capacitance

The EDLC electrode was prepared by mixing of AC, acetylene black, and polytetrafluoroethylene (PTFE) at a weight ratio of 87:10:3 using an agate mortar and then pressed onto an aluminum mesh current collector at 10 kg cm^{-2}. The diameter of the electrode was 13 mm. After dried in vacuum at 200 °C for 2 h, two of the electrodes were assembled at room temperature in a clean and dry Ar atmosphere into a hermetic aluminum Hohsen HS Test Cell and filled with 0.5 M TEABF$_4$/PC as electrolyte. The galvanostatic charge/discharge test of the EDLC electrode was performed between 0 and 2.5 V using a Hokuto Denko HJ1001SM8A battery charge/discharge unit under a constant current density of 10 mA g^{-1}. Capacitance was deduced from the formula $C = Idt/dV$, where I is the discharge current density (mA g^{-1}), dt is the discharge time variation, and dV is the voltage variation in discharge [20,21].

3. Results and discussion

3.1. KOH and NaOH activation

3.1.1. Structural characterization of ACs

As exhibited in Fig. 1, the isotherms are type I according to the IUPAC classification [22]. The nitrogen adsorption major occurs at a relative pressure less than 0.3. A relatively horizontal adsorption plateau appears at the high P/P_0 value, indicating that the micropores are dominant in the resulting ACs. As can be deduced from Fig. 2, the pore diameters of the two series of ACs are about 0.6–1 nm. At the same time, it can be observed that the ACs activated with NaOH exhibit larger adsorption volume than that with KOH at both low and high relative pressures.

As Table 1 shows, at 600 and 700 °C, the adsorption capacity and the TPV of the AC obtained from NaOH activation are more considerable than that from KOH activation, although KOH activation leads to a higher AC yield than NaOH activation. In addition, the porosity distributions of the ACs prepared by KOH activation show narrower microporous distributions than those prepared by NaOH activation. As can be deduced from Table 1, the SSA of ACs covers a very wide range from 1261 m^2 g^{-1} up to higher than 3000 m^2 g^{-1}. It is worth emphasizing that Na4-700 reached a SSA of 3010 m^2 g^{-1} and a TPV of 1.77 cm^3 g^{-1}. Generally, NaOH and KOH are interestingly stable chemicals that melt without decomposition at 318 and 360 °C, respectively [23]. At a high temperature, both the alkaline hydroxides can react with most of the precursors, even with the quite inert carbon materials. The redox reaction between precursors and alkaline hydroxides (both NaOH and KOH) causes the conversion to hydrogen, alkaline metals and alkaline carbonates [24–26]. During this reaction, the number of pores of the carbon precursor is increased considerably, as well as the size of the existing ones. Hence, it can prepare ACs in high SSA containing an enormous amount of micropores and small mesopores via this hydroxide-carbon reaction.

As shown in Fig. 3, when raising the temperature from 500 to 700 °C, the SSA of the ACs obtained from KOH and NaOH activations increased and reached the maximum values of 2594 and 3010 m^2 g^{-1}, respectively.

Table 1
Characteristics of the ACs.

Sample	AT (°C)	Reagent	Ratio	Y_c (%)	Y_{total} (%)	S_{BET} (m^2 g^{-1})	V_{total} (m^3 g^{-1})	D_{ave} (nm)	C_g (F g^{-1})	C_v (F cm^{-3})
K4-500	500	KOH	4	69.3	58.2	1186	0.55	1.77	29.2	20.0
K4-600	600	KOH	4	69.3	46.8	2171	1.10	1.79	39.5	22.5
K4-700	700	KOH	4	69.3	43.6	2594	1.36	1.84	43.1	20.1
K4-800	800	KOH	4	69.1	38.6	2447	1.46	1.92	42.5	17.9
Na4-500	500	NaOH	4	71.1	54.6	1261	0.55	1.99	26.9	19.0
Na4-600	600	NaOH	4	70.6	32.9	2922	1.62	1.91	42.5	21.8
Na4-700	700	NaOH	4	70.6	32.0	3010	1.77	1.99	43.9	20.2
Na4-800	800	NaOH	4	70.6	27.6	2007	1.27	2.03	42.8	18.6
K2-700	700	KOH	2	68.7	50.3	1834	0.79	1.88	34.6	20.6
K2-800	800	KOH	2	68.7	42.4	2378	1.12	1.77	40.8	21.2
K2-900	900	KOH	2	68.7	31.9	1545	0.85	2.08	34.5	18.7
Ca2-700	700	$CaCO_3$	2	68.1	56.4	30	0.02	3.13	0.38	0.34
Ca2-800	800	$CaCO_3$	2	68.1	53.6	11	0.01	2.83	0.35	0.33
Ca2-900	900	$CaCO_3$	2	68.1	52.3	15	0.01	3.42	0.32	0.30
K2Ca2-700	700	KOH/$CaCO_3$	2/2	69.9	50.4	643	0.31	1.93	12.7	9.6
K2Ca2-800	800	KOH/$CaCO_3$	2/2	69.9	42.4	988	0.49	1.92	16.4	11.5
K2Ca2-900	900	KOH/$CaCO_3$	2/2	69.9	21.8	566	0.30	1.98	13.4	10.1

AT: activation temperature; Y_c: char yield; Y_{total}: total yield; C_g: gravimetric specific capacitances; C_v: volumetric specific capacitances.
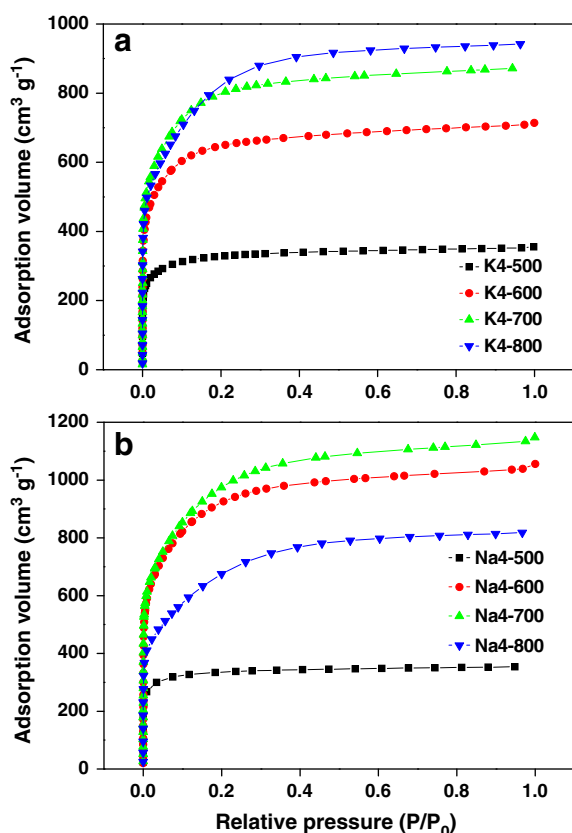
Fig. 1. Nitrogen adsorption isotherms of the ACs from KOH (a) and NaOH (b) activations.
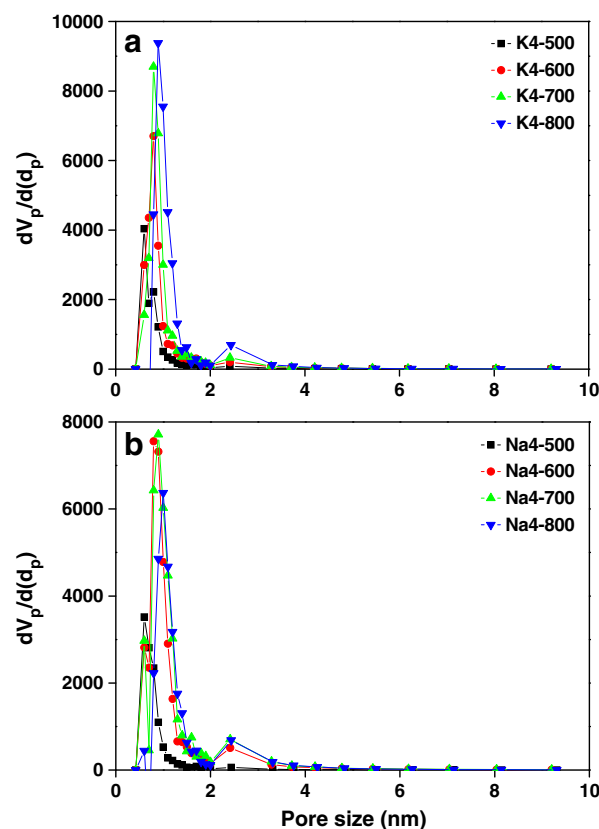

Fig. 2. Pore distribution of ACs from KOH (a) and NaOH (b) activations.

KOH activation of biomass wastes [17,27] also gave a similar increasing trend in the SSA of the ACs with rising activation temperature. Azargohar and Dalai [17] proposed that the increase in porosity was due to the enhancement of creation of new pores from the reaction between char and KOH or NaOH with the rising temperature. Further raising the temperature to 800 °C led to the decrease in SSA, especially for Na4-800, which should be due to the severe activation at high temperatures that has a detrimental impact on the development of porosity on ACs. At a temperature range from 500 to 700 °C, the porosity development of ACs prepared from NaOH activation is better than those from KOH activation. However, this trend changes when further raising activation temperature to 800 °C, during when a significant decrease in SSA of the Na4-800 can be found. Therefore, ACs prepared with NaOH activation should not exceed 700 °C.

As mentioned above, the representative AC of K4-700 possessed both high SSA and TPV. TEM was used to further study the porous texture of the AC, detailed in Fig. 4. Apparently, K4-700 consists of small particles, as shown in Fig. 4a. The particles connect to each other and form an aggregate in irregular shapes. This structure appeared on the surface of the K4-700 when activation was carried out with a certain amount of KOH. This trend suggested that the pyrolysis and etching process occurred simultaneously during the activation. In addition, an obvious graphitic structure can also be observed after the KOH treatment. As appeared in Fig. 4b, it should be noticed that the amorphous carbon in a turbostratic structure can be observed in K4-700.

3.1.2. Electrochemical performances of the ACs

Galvanostatic charge–discharge measurements were carried out to examine the electrochemical performances of the obtained porous carbons. From Fig. 5, it can be seen that the charge–discharge curves of the ACs are closely linear with a small deviation from ideal voltage–time curves, which may be associated with the internal resistance during the changing of polarity [28]. As listed in Table 1, the gravimetric specific

capacitance of K4-700 and Na4-700 reached 43.1 and 43.9 F g^{-1}, respectively. Meanwhile both the ACs owed the highest SSA. It should be noted that the SSA of Na4-700 (3010 m^2 g^{-1}) is significantly greater than K4-700 (2594 m^2 g^{-1}). However, the capacitance of Na4-700 is only slightly higher than K4-700. This observation may be explained by restriction accessibility of electrolyte ions to the pores or the surface of ACs was not completely wetted, leading to the partial utilization of the SSA. The double layer capacitance is correlated with the morphological property of the porous electrode, such as the SSA and the pore size distribution of the ACs [29]. Pores that are too large or too small can reduce the density of the electrode and keep the electrolyte out of the pores, respectively [30]. Thus, tailoring the porous structure of the carbon material is a major goal for EDLC optimization. As presented in Fig. 6, it can be
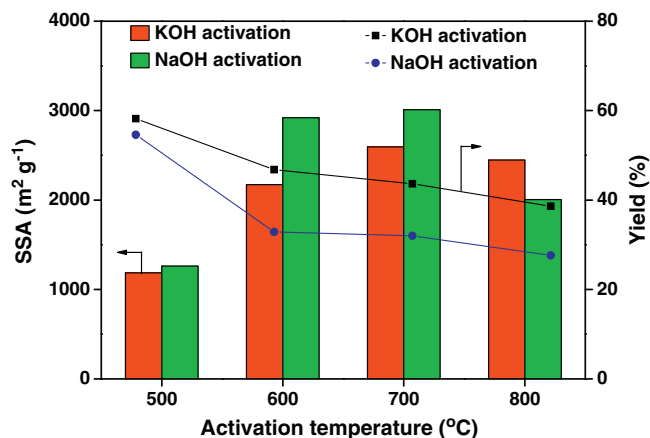

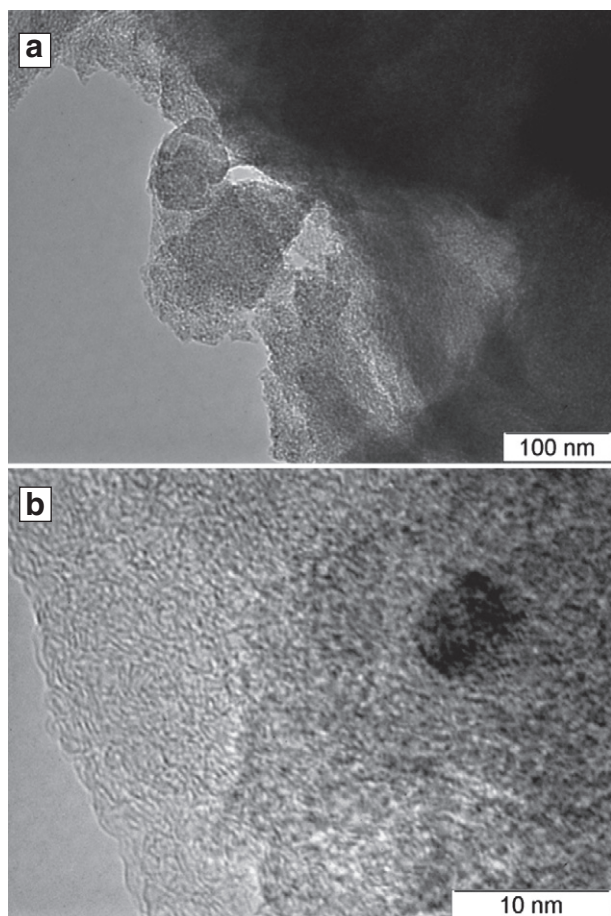**Fig. 3.** SSA and yield of ACs at different temperatures.

Fig. 4. TEM images of K4-700 at low- (a) and high-resolution (b).

Fig. 5. Charge–discharge curves of AC electrodes from KOH (a) and NaOH (b) activations.

observed that a similar tendency was achieved by NaOH and KOH activations, whereas NaOH shows higher specific capacitances than KOH at 600–800 °C.

It is interesting that the SSA of K4-600 and Na4-600 (2171 and 2922 m^2 g^{-1}) are smaller than K4-700 and Na4-700 (2594 and 3010 m^2 g^{-1}), whereas the volumetric specific capacitance of K4-600 and Na4-600 (22.5 and 21.8 F cm^{-3}) is larger than that of K4-700 and Na4-700 (20.1 and 20.2 F cm^{-3}). Such excellent electrochemical performance of K4-600 and Na4-600 illustrates that the ACs activated at 600 °C should have more accessible SSA for the formation of an electric double layer. Some researchers proved that the higher capacitance per volume must be obtained with pores of right size which can adsorb the larger amount of electrolyte on their wall with lower amount of unadsorbed electrolyte in the same pore [31]. The relatively high volumetric capacitance of K4-600 and Na4-600 should be due to the enhanced accessibility of the electrolyte ions to a suitable pore size. Similar trend was reported for black liquor- [27] and corncob-derived ACs [28].

Consequently, NaOH activation can achieve almost the same performance as KOH activation, such as total yield, SSA, and specific capacitance. Although KOH and NaOH can be used interchangeably in a large number of applications, NaOH was emphasized especially here in regard to its low cost and corrosive.

3.2. HyperCoal activated with $CaCO_3$ and $KOH/CaCO_3$ mixture

3.2.1. Structural characterization of ACs

HyperCoal was activated with $CaCO_3$ at 700–900 °C for 2 h under Ar flow in a $CaCO_3$/char ratio of 2. For comparison, activation of HyperCoal char with the same amount of KOH and $KOH/CaCO_3$ mixture was also carried out in the same manner. As exhibited in Fig. 7, it can be observed

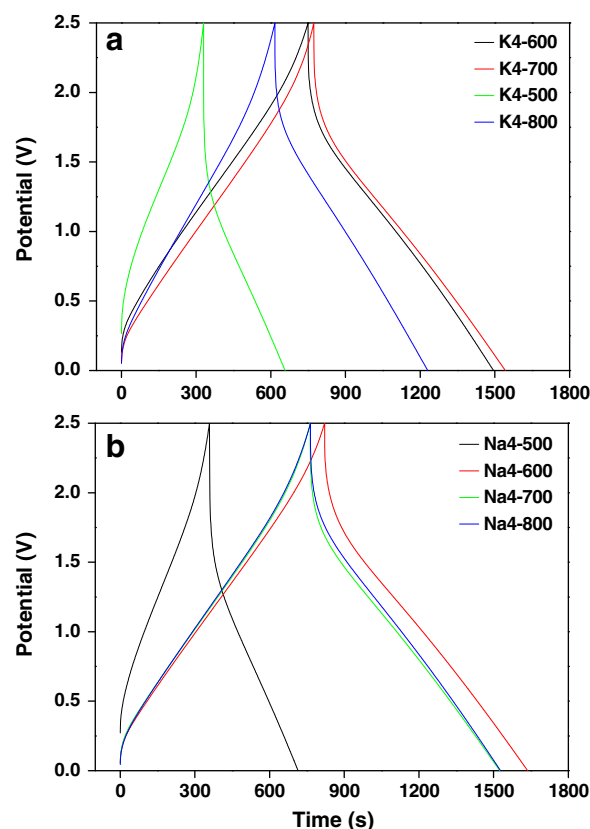that the isotherms belong to type I for micropore materials activated with KOH and $KOH/CaCO_3$ mixture according to the IUPAC classification, as shown in Fig. 7a and c. In the case of ACs from $CaCO_3$ activation (Fig. 7b), the isotherms were similar to type I and IV according to the IUPAC classification [22]. The adsorption isotherms rapidly increased in the region of middle and high relative pressure and no platform appeared, indicating that the ACs might contain mesopores, which can be further proved in Fig. 8. From Fig. 8b, it can be seen that there are three peaks with pore sizes of 0.5–1, 1–2, and 2–4 nm, which is well consistent with the adsorption isotherms.

As shown in Fig. 9, the ACs from $CaCO_3$ activation at 700–900 °C showed an SSA value of 11–30 m^2 g^{-1}. $CaCO_3$ practically has an unfavorable effect on porosity development. In contrast, KOH with the same mass ratio of 2:1 provided a large SSA of around 2400 m^2 g^{-1} at 800 °C.
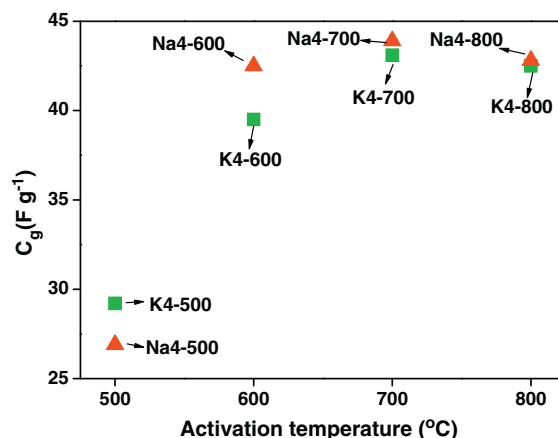

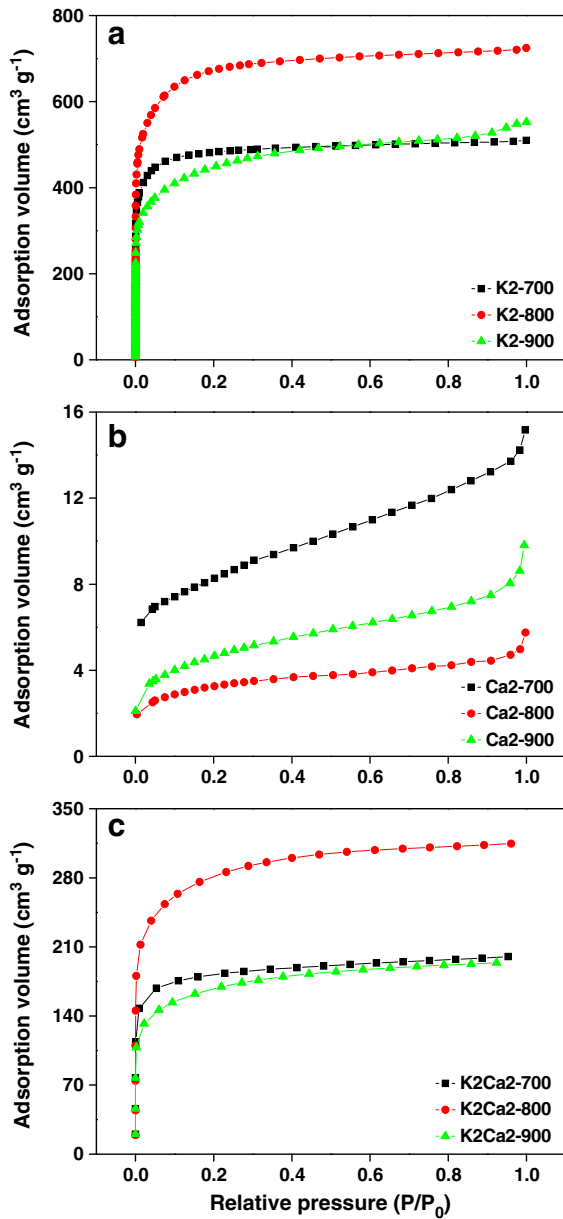Fig. 6. Specific capacitances of the ACs from NaOH and KOH activations.

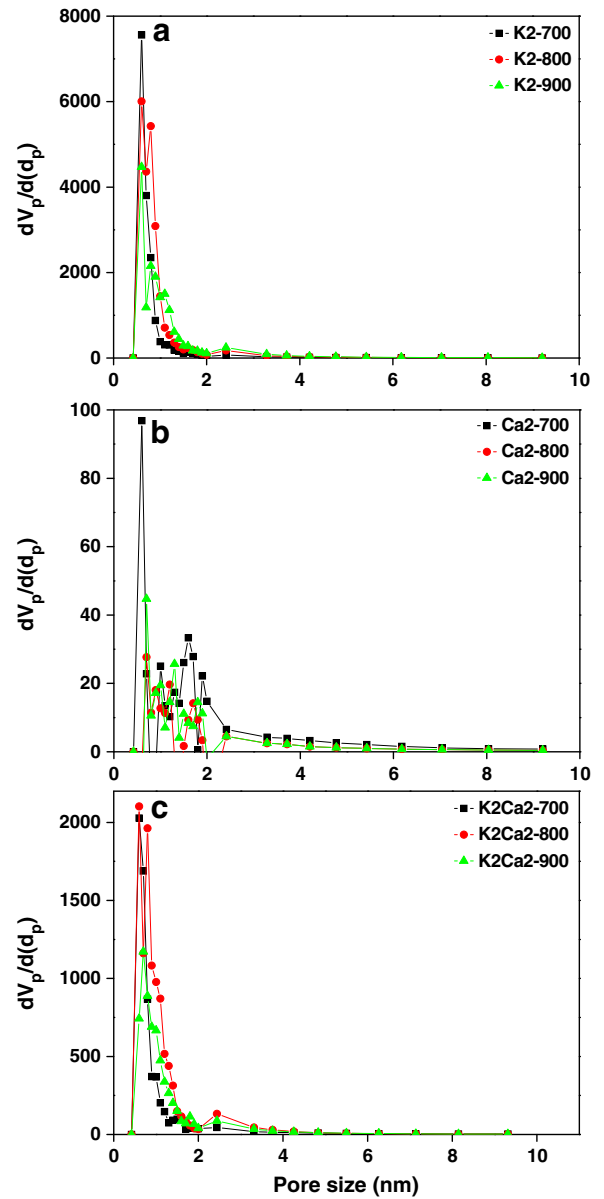**Fig. 7.** Nitrogen adsorption isotherms of the ACs from KOH (a), CaCO$_3$ (b), and KOH/CaCO$_3$ mixture (c) activations.

Fig. 8. Pore distribution of ACs from KOH (a), CaCO$_3$ (b), and KOH/CaCO$_3$ mixture (c) activations.

Nevertheless, the SSA decreased to 988 m^2 g^{-1} when CaCO$_3$ was added for KOH activation at the same temperature. The same phenomenon also occurs in the temperature below or above 800 °C. Therefore, it can be concluded that CaCO$_3$ activation does not play a role in physical activation to increase the amount of micropores for providing high SSA AC as expected. Furthermore, CaCO$_3$ has an inhibitory effect on the KOH activation to a certain extent. It should be noted that CaCO$_3$ activation could give a high yield of ACs around 50%, whereas the yields from KOH and KOH/CaCO$_3$ activations were around 40%. Activation with the KOH/CaCO$_3$ mixture above 800 °C reduced the yield sharply.

3.2.2. Electrochemical performances of the ACs

As shown in Table 1, the gravimetric specific capacitances of ACs obtained from CaCO$_3$ activation are lower than 1 F g^{-1}. In contrast, KOH activation provided ACs with high specific capacitance and reached an acceptable value of 40.8 F g^{-1} at 800 °C. However, further raising the activation temperature to 900 °C reduced the capacitance of the ACs. As expected, adding CaCO$_3$ during KOH activation significantly decreased
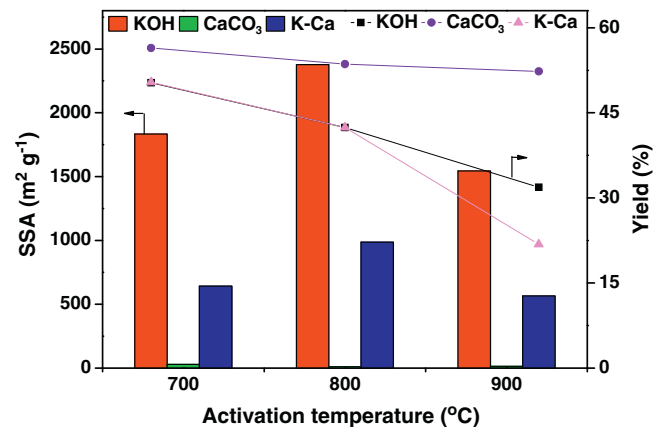

Fig. 9. SSA and yields of ACs at different temperatures.

the specific capacitance (below 20 F g^{-1}). AC with a large SSA was considered to be a basic guiding principle for large capacitance electrode production [31,32].

Although the BET method plays an important role in porous materials, it is a restriction to analyze the SSA with different pore size ranges. In general, the porous AC for EDLC electrode usually has relatively high SSA and unique porous structure [33–35]. The non-accessible pores have little contribution to the capacitance, and an excessively large pore size will also produce non-accessible pores [27]. Yet, CaCO$_3$ as an activating agent gave an AC with relatively low SSA and TPV, as well as a low specific capacitance. In this study, the AC obtained from the CaCO$_3$/KOH mixture activation presents a certain number of mesopores, which has little contribution to the capacitance, resulting in a relatively low specific capacitance. As listed in Table 1, the average pore size of ACs activated with KOH and KOH/CaCO$_3$ mixture concentrated in 1–2 nm, while those from CaCO$_3$ activation are larger than 2 nm. The AC with a relatively narrow pores (1–2 nm) shows a higher specific capacitance than that with mesopores (>2 nm). It is implied that the contribution of the pores in 1–2 nm to the performance of EDLC is higher than the pores above 2 nm. This trend is well consistent with the results reported [36]. As displayed in Fig. 10, the discharge times of the K2-800 electrode is much longer than that of Ca2-800 and K2Ca2-800 electrodes, indicating that the specific capacitances of the ACs are remarkably enhanced by the KOH activation and CaCO$_3$ is not suitable for the preparation of high-performance AC electrode. Simultaneously, their plots present good linearity and symmetrical triangle, indicating good EDLC behaviors.

As discussed above, the SSA and the specific capacitance of ACs from KOH activation are higher than the other two series ACs. The sharp reduction in capacitance reflects that CaCO$_3$ does not play the same role as CO$_2$ activation for developing pores and is not beneficial for the properties of the resulting ACs. Consequently, the CaCO$_3$ content should be significantly reduced when coal was used as a precursor for high-performance AC preparation.

4. Conclusions

The ACs with SSA of 2594 and 3010 m^2 g^{-1} and TPV of 1.36 and 1.77 cm^3 g^{-1} were produced from carbonization and activation of HyperCoal with KOH and NaOH, respectively. The ACs obtained from KOH and NaOH activations at 700 °C exhibit the highest specific capacitances of 43.1 and 43.9 F g^{-1}, respectively, at a current density of 10 mA g^{-1} in 0.5 M TEABF$_4$/PC electrolyte. The AC electrodes exhibited good charge–discharge performance. Meanwhile, the ACs prepared by CaCO$_3$ and KOH/CaCO$_3$ mixture activations, which have SSA of 30 and 988 m^2 g^{-1} and TPV of 0.02 and 0.49 cm^3 g^{-1}, respectively, resulted in

quite low capacitance. CaCO$_3$ significantly inhibits the pore development during KOH activation and is not beneficial for high specific capacitance AC preparation. The electrochemical performance of the ACs significantly depended on the SSA and the pore size distribution. Such an approach may lead to the development of high-performance EDLC electrodes from HyperCoal.

References

[1] M.J. Jung, E. Jeong, Y. Kim, Y.S. Lee, Influence of the textual properties of activated carbon nanofibers on the performance of electric double-layer capacitors, Journal of Industrial and Engineering Chemistry 19 (2013) 1315–1319.
[2] A. Davies, A.P. Yu, Material advancements in supercapacitors: from activated carbon to carbon nanotube and graphene, Canadian Journal of Chemical Engineering 89 (2011) 1342–1357.
[3] C. Peng, X.B. Yan, R.T. Wang, J.W. Lang, Y.J. Ou, Q.J. Xue, Promising activated carbons derived from waste tea-leaves and their application in high performance supercapacitors electrodes, Electrochimica Acta 87 (2013) 401–408.
[4] H. Zhang, G.P. Cao, Y.S. Yang, Carbon nanotube arrays and their composites for electrochemical capacitors and lithium-ion batteries, Energy & Environmental Science 2 (2009) 932–943.
[5] V. Barranco, M.A. Lillo-Rodenas, A. Linares-Solano, A. Oya, F. Pico, J. Ibanez, F. Agullo-Rueda, J.M. Amarilla, J.M. Rojo, Amorphous carbon nanofibers and their activated carbon nanofibers as supercapacitor electrodes, Journal of Physical Chemistry C 114 (2010) 10302–10307.
[6] J. Yan, T. Wei, B. Shao, F.Q. Ma, Z.J. Fan, M.L. Zhang, C. Zheng, Y.C. Shang, W.Z. Qian, F. Wei, Electrochemical properties of graphene nanosheet/carbon black composites as electrodes for supercapacitors, Carbon 48 (2010) 1731–1737.
[7] M.A. Lillo-Ródenas, D. Cazorla-Amorós, A. Linares-Solano, Understanding chemical reactions between carbons and NaOH and KOH: an insight into the chemical activation mechanism, Carbon 41 (2003) 267–275.
[8] D. Lozano-Castello, J.M. Calo, D. Cazorla-Amorós, A. Linares-Solano, Carbon activation with KOH as explored by temperature programmed techniques, and the effects of hydrogen, Carbon 45 (2007) 2529–2536.
[9] S. Murali, D.R. Dreyer, P. Valle-Vigón, M.D. Stoller, Y. Zhu, C. Morales, A.B. Fuertes, C.W. Bielawski, R.S. Ruoff, Mesoporous carbon capsules as electrode materials in electrochemical double layer capacitors, Physical Chemistry Chemical Physics 13 (2011) 2652–2655.
[10] X.J. He, P.H. Ling, M.X. Yu, X.T. Wang, X.Y. Zhang, M.D. Zheng, Rice husk-derived porous carbons with high capacitance by ZnCl$_2$ activation for supercapacitors, Electrochimica Acta 105 (2013) 635–641.
[11] Z. Shen, R. Xue, Preparation of activated mesocarbon microbeads with high mesopore content, Fuel Processing Technology 84 (2003) 95–103.
[12] Z.H. Feng, R.S. Xue, X.H. Shao, Highly mesoporous carbonaceous material of activated carbon beads for electric double layer capacitor, Electrochimica Acta 55 (2010) 7334–7340.
[13] L. Wei, G. Yushin, Nanostructured activated carbons from natural precursors for electrical double layer capacitors, Nano Energy 1 (2012) 552–565.
[14] A. Elmouwahidi, Z. Zapata-Benabithe, F. Carrasco-Marín, C. Moreno-Castilla, Activated carbons from KOH-activation of argan (argania spinosa) seed shells as supercapacitor electrodes, Bioresource Technology 111 (2012) 185–190.
[15] D. Liu, J. Shen, N.P. Liu, H.Y. Yang, A. Du, Preparation of activated carbon aerogels with hierarchically porous structures for electrical double layer capacitors, Electrochimica Acta 89 (2013) 571–576.
[16] K. Sato, S. Suemune, K. Nitta, C. Nakayama, S. Inokuma, S. Tonooka, Y. Mamada, E. Nakamura, K. Kaneko, K. Takarada, A simple fabrication route of activated carbons from chicken droppings, Journal of Analytical and Applied Pyrolysis 101 (2013) 86–89.
[17] R. Azargohar, A.K. Dalai, Steam and KOH activation of biochar: experimental and modeling studies, Microporous Mesoporous Mater 110 (2008) 413–421.
[18] N. Okuyama, N. Komatsu, T. Shigehisa, T. Kaneko, S. Tsuruya, Hyper-coal process to produce the ash-free coal, Fuel Processing Technology 85 (2004) 947–967.
[19] X.Y. Zhao, S.S. Huang, J.P. Cao, S.C. Xi, X.Y. Wei, J. Kamamoto, T. Takarada, KOH activation of a HyperCoal to develop activated carbons for electric double-layer capacitors, Journal of Analytical and Applied Pyrolysis 105 (2014) 116–121.
[20] S.H. Kwon, E. Lee, B.S. Kim, S.G. Kim, B.J. Lee, M.S. Kim, J.C. Jung, Activated carbon aerogel as electrode material for coin-type EDLC cell in organic electrolyte, Current Applied Physics 14 (2014) 603–607.
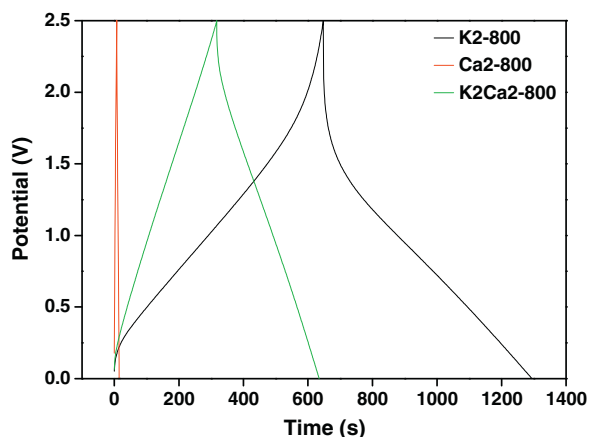

Fig. 10. Charge–discharge curves of AC electrodes activated with KOH, CaCO$_3$, and KOH/CaCO$_3$ mixture.

[21] Q. Li, R.R. Jiang, Y.Q. Dou, Z.X. Wu, T. Huang, D. Feng, J.P. Yang, A.S. Yu, D.Y. Zhao, Synthesis of mesoporous carbon spheres with a hierarchical pore structure for the electrochemical double-layer capacitor, Carbon 49 (2011) 1248–1257.

[22] F. Rouquerol, J. Rouquerol, S. Kenneth, Is the BET Equation Applicable to Microporous Adsorbents Adsorption by Powders and Porous Solids, Academic Press, London, 1999.

[23] A. Linares-Solano, M.A. Lillo-Ródenas, J.P. Marco-Lozar, M. Kunowsky, A.J. Romero-Anaya, NaOH and KOH for preparing activated carbons used in energy and environmental applications, International Journal of Energy, Environment and Economics 20 (2012) 59–91.

[24] D.W. McKee, Gasification of graphite in carbon dioxide and water vapor-the catalytic effects of alkali metal salts, Carbon 20 (1982) 59–66.

[25] A. Perrina, A. Celzarda, A. Albiniakb, J. Kaczmarczykb, J.F. Marêchéa, G. Furdina, NaOH activation of anthracites: effect of temperature on pore textures and methane storage ability, Carbon 42 (2004) 2855–2866.

[26] E. Fuentea, R.R. Gila, R.P. Giróna, M.A. Lillo-Ródenasb, M.A. Montes-Morána, M.J. Martinc, A. Linares-Solano, Evidence for the presence of cyanide during carbon activation by KOH, Carbon 48 (2010) 1032–1037.

[27] X.Y. Zhao, J.P. Cao, K. Morishita, J.-i. Ozaki, T. Takarada, Electric double-layer capacitors from activated carbon derived from black liquor, Energy & Fuels 24 (2010) 1889–1893.

[28] L.L. Ding, B. Zou, H.Q. Liu, Y.N. Lia, Z.C. Wang, Y. Su, Y.P. Guo, X.F. Wang, A new route for conversion of corncob to porous carbon by hydrolysis and activation, Chemical Engineering Journal 225 (2013) 300–305.

[29] O. Barbieri, M. Hahn, A. Herzog, R. K tz, Capacitance limits of high surface area activated carbons for double layer capacitors, Carbon 43 (2005) 1303–1310.

[30] S.S. Mitani, S.I. Lee, K. Saito, S.H. Yoon, Y. Korai, I. Mochida, Activation of coal tar derived needle coke with K_2CO_3 into an active carbon of low surface area and its performance as unique electrode of electric double-layer capacitor, Carbon 43 (2005) 2960–2967.

[31] S. Mitani, S.I. Lee, S.H. Yoon, Y. Korai, I. Mochida, Activation of raw pitch coke with alkali hydroxide to prepare high performance carbon for electric double layer capacitor, Journal of Power Sources 133 (2004) 298–301.

[32] B. Xu, F. Wu, R.J. Chen, G.P. Cao, S. Chen, Z.M. Zhou, S.Y. Yang, Highly mesoporous and high surface area carbon: a high capacitance electrode material for EDLCs with various electrolytes, Electrochemistry Communications 10 (2008) 795–797.

[33] K. Xia, Q. Gao, J. Jiang, J. Hu, Hierarchical porous carbons with controlled micropores and mesopores for supercapacitor electrode materials, Carbon 46 (2008) 1718–1726.

[34] R.Q. Sun, L.B. Sun, Y. Chun, Q.H. Xu, Catalytic performance of porous carbons obtained by chemical activation, Carbon 46 (2008) 1757–1764.

[35] M. Sevilla, R. Mokaya, A.B. Fuertes, Ultrahigh surface area polypyrrole-based carbons with superior performance for hydrogen storage, Energy & Environmental Science 4 (2011) 2930–2936.

[36] C. Largeot, C. Portet, J. Chmiola, P.L. Taberna, Y. Gogotsi, P. Simon, Relation between the ion size and pore size for an electric double-layer capacitor, Journal of the American Chemical Society 130 (2008) 2730–2731.